Protection of organic matter by mineral matrix in a Cenomanian black shale

V. Salmon, Sylvie Derenne, Elisabeth Lallier-Vergès, Claude Largeau, Bernard Beaudoin

Protection of organic matter by mineral matrix in a Cenomanian black shale

V Salmon[a,b] S Derenne[a] E Lallier-Vergès[c], C Largeau[a], B Beaudoin[b]

[a] UMR CNRS 7573, Laboratoire de Chimie Bioorganique et Organique Physique, Ecole Nationale Supérieure de Chimie de Paris, 75231 Paris Cedex 05, France

[b] Laboratoire de Sédimentologie, Ecole des Mines de Paris, 77205 Fontainebleau Cedex, France. Depuis ISTO UMR6113 puis UMR 7327

[c] UMR CNRS 6531, Laboratoire de Géologie de la Matière Organique, Université d'Orléans, 45067 Orléans Cedex, France

Abstract

Three types of pathways (degradation–recondensation, natural sulphurization and selective preservation) are commonly considered for the formation of kerogen dispersed in sedimentary rocks. A fourth pathway has been recently put forward, however, from studies on Recent marine sediments, the so-called sorptive protection mechanism. This pathway is based on the adsorption of otherwise labile organic compounds onto minerals, thus preventing their diagenetic degradation and promoting their subsequent condensation into kerogen. The main results of the present study are derived from a combination of microscopic and pyrolytic methods applied on a Cenomanian kerogen. They provide (i) evidence, on an ancient material, for a crucial role of the mineral matrix both in organic matter (OM) preservation during kerogen formation and in kerogen stability once formed, (ii) indications that the dominant protective process likely involves physical protection by minerals, resulting from alternation of organic and clay nanolayers of approximately 100 nm in thickness, rather than OM adsorption as molecular monolayers and (iii) observations of the relatively poor stability of an isolated kerogen, contrary to the inertness commonly assumed for fossil macromolecular organic matter.

Keywords

- Mineral protection;
- Kerogen stability;
- SEM BSE;
- TEM;
- Pyrolysis

1. Introduction

Several mechanisms are commonly considered to explain OM accumulation in sedimentary rocks. In addition to the first recognized process of OM preservation, the classical degradation–recondensation pathway as defined by Tissot and Welte (1984), two other mechanisms have been extensively studied and are now well understood, namely the selective preservation (e.g. Tegelaar et al., 1989) and the natural sulphurization (e.g. Sinninghe Damsté et al., 1989) pathways. Recently, a new mechanism has been proposed, involving a protective role by minerals: the so-called sorptive protection pathway. Indeed, a textural control of

organic matter concentration has been previously suggested by studies showing that total organic carbon (TOC) content increases when the mean particle size of the sediment decreases (Mayer et al, 1985, Suess 1973 and Tanoue & Handa 1979). This hypothesis was further supported by correlations between TOC and surface areas of mineral grains in various coastal sediments (Bergamashi et al., 1997, Keil et al., 1994a, Keil et al., 1994b, Mayer et al., 1988, Mayer 1994a and Mayer 1994b). Such correlations were ascribed to a monolayer adsorption of organic compounds onto minerals. Considering that more than 80% of sediment surface area is accounted for by the interiors of 2 to 8 nm wide pores on mineral surfaces, it was concluded that most of the organic matter was concentrated in these pores (Mayer 1994a and Mayer 1994b). In addition to a physical protection from biodegradation (e.g. the small size of the pores excludes hydrolytic enzymes), OM adsorption into pores should favour subsequent condensation reactions by concentrating the reactants (Collins et al., 1995). In addition, some minerals (i.e. clays) are known to have catalytic properties (Degens and Ittekkot, 1984). Recently Ransom 1997, Ransom et al, 1998a and Ransom 1998b have contested the sorptive hypothesis and many questions, such as the distribution of OM on mineral surfaces, remain unanswered. Moreover, as stressed by Collins et al. (1995), all the above studies dealt only with recent sediments.

The aims of this work were to study the relationship between OM and the mineral matrix in a Cenomanian black shale and to study the role of this matrix in OM preservation. To this end, the black shale was examined at different scales (microscopic to nanoscopic) using natural light and UV fluorescence microscopy on thin sections, back-scattered scanning electron microscopy (SEM BSE) on polished sections, and transmission electron microscopy (TEM) on ultrathin sections. The stability upon storage of the organic matter, once isolated from its mineral matrix, was also investigated.

The black shale sample was collected in the Umbria-Marche Basin, Central Italy. In this basin, the upper part of the Cenomanian is characterized by the cyclic deposition, lasting about 2.5 Myears, of black shales and cherts in carbonate sediments. This cyclicity has been related to the precessional motion of the Earth (Beaudoin et al., 1996). The well-known organic-rich “Bonarelli horizon” that underlines the Cenomanian/Turonian boundary (~93.3 Ma) represents the final term of this series. This level corresponds to one of the most conspicuous oceanic anoxic events (OAE), as defined by Schlanger and Jenkyns (1976), that occurred on a global scale during this period.

Our study is focused on an organic-rich (TOC=13.6 wt%, Hydrogen Index=454 mg HC/g TOC) sample taken from an immature black shale layer outcropping 12 m below the “Bonarelli horizon”. A preliminary chemical study (Salmon et al., 1997) on this sample revealed: (i) OM of dominantly marine origin, (ii) a low organic sulphur content, showing that natural sulphurization was not largely implicated in the formation of this kerogen and (iii) a low level of degradation of incorporated lipids, indicating that the classical degradation-recondensation pathway was unlikely to be important. Observations using light microscopy on the OM, isolated from the whole rock by acid attacks, showed a dominantly amorphous material along with few ligno-cellulosic debris (at most 5% of the total kerogen based on surface estimations) and morphologically preserved debris likely of marine origin (~1%). Transmission electron microscopy studies of the isolated kerogen showed that the bulk of the OM did not retain any morphological features of the source organisms. This amorphous character, at a nanoscopic scale, pointed to a negligible role for the selective preservation pathway. Taken together, the above observations therefore suggested that among the four recognized pathways the fourth one, i.e. sorptive protection, could be the main process

responsible for the formation of this organic-rich level. Further studies presented here were thus performed to test this hypothesis and to examine the role of the mineral matrix in OM preservation in this black shale.

2. Experimental

2.1. Samples

The black shale sample, previously described in Salmon et al. (1997), was collected from a clay-rich layer. A small amount of this sample was directly used for petrographic observations and the remaining material was ground for further analyses. Rock-Eval pyrolysis was performed on the ground material. Thereafter, the ground rock was extracted with organic solvents (CHCl3/MeOH, 2/1, v/v) and a part was subjected to classical HF/HCl treatment for kerogen isolation (Durand and Nicaise, 1980). One fraction of this kerogen (ker-0) was immediately analysed by spectroscopic methods (FTIR and solid state ^{13}C NMR) and submitted to molecular analysis via pyrolysis. A second and a third fraction of this kerogen were similarly analysed but after one (ker-1) and two (ker-2) years of storage in a closed vessel, in darkness, at room temperature. The remaining part of the ground bitumen-free rock was stored in a closed vessel for two years, also in darkness, and at room temperature before isolating the kerogen (ker-2bis). The flow chart summing up the preparation of these different kerogen fractions is shown in Fig. 1.

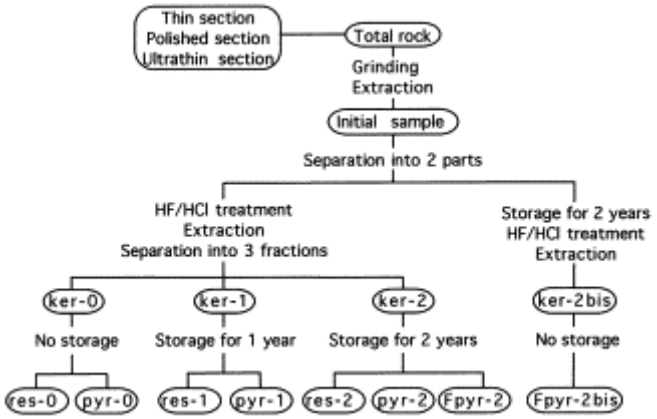

Fig. 1. Flow chart illustrating the preparation of the different kerogen samples analysed, derived pyrolysates (pyr- and Fpyr- correspond to off-line and on-line experiments, respectively) and pyrolysis residues (res-).

2.2. Petrographic studies

Petrographic studies were performed on the total rock for all the observation modes. Thin sections of the black shale were examined using transmitted light (natural light and UV excitation) with a Leitz MPVII microscope. SEM BSE was carried out on polished sections, embedded in epoxy resin to ensure sample cohesion, with a JEOL JSM 6400 scanning electron microscope, coupled with a KEVEX probe allowing for elemental mapping and pin-point analysis. Ultra-thin sections were prepared for TEM observation according to Boussafir et al, 1994 and Boussafir et al., 1995). TEM study for whole rock observations requires several preparation stages. First, selected small rock fragments perpendicular to the bedding

plane were fixed with OsO_4. Then these fragments were dipped in acetone-resin mixtures at progressively increasing resin concentration in order to allow for the penetration of the embedding resin. Once embedded, they were observed under natural light and UV excitation to select the zones to be studied (representative zones of the bulk organic material, i.e. with intimate associations between clays and organic matter). These zones were circled and then pyramids for ultra-thin sections were prepared from the circled zones. Then, ultra-thin sections were cut on pre-selected zones perpendicular to the bedding plane. Ultra-thin sections obtained with a diamond knife were observed using a JEOL 100CX TEM. Differentiation between organic matter, resin, membrane from the sample holder and void space has been performed by the recognition of zones where two or three of these features occur, enabling a grey level to be assigned describing the nature of the observed object. High resolution TEM studies (HRTEM), electron micro-diffraction and X-ray analysis (EDAX) were additionally performed on the clay minerals using a CM 20 Philips TEM.

2.3. Bulk chemical measurements

Rock-Eval analyses were performed on 30–50 mg of ground rock using a Rock-Eval 6 with a temperature program from 300°C (20 min) to 600°C at 25°C/min under an He flow. All the other analyses were performed on the isolated kerogen samples prepared as described in Fig. 1.

FTIR spectra were recorded with a Bruker IFS48 spectrometer as KBr pellets. The ^{13}C NMR spectra of the isolated kerogen stored for two years (ker-2) and of the kerogen isolated from the ground rock stored for two years (ker-2bis) were recorded on a Bruker MSL 400 under the same conditions as described in Salmon et al. (1997).

2.4. Off-line and flash pyrolysis

Off-line pyrolysis under a helium flow was performed as described in Largeau et al. (1986). Briefly, it consists of the volatilization of the thermolabile compounds by heating at 300°C for 20 min, followed by cracking at 400°C for 1 h. The pyrolysis products, thus generated, were trapped in chloroform at −5°C and the solvent evaporated to dryness under vacuum. The pyrolysate was then separated by column chromatography with three solvents of increasing polarity, *n*-heptane, toluene and methanol. The methanol-eluted fraction was then esterified in order to enhance fatty acid detection. Each fraction was finally analysed by combined gas chromatography/mass spectrometry (GC/MS). The GC/MS analyses were carried out on a Hewlett-Packard 5890 Serie II gas chromatograph — equipped with a 25 m CP Sil 5 CB capillary column (i.d. 0.25 mm, film thickness 0.4 μm) programmed from 100 to 300°C at 4°C/min — coupled with a Hewlett-Packard 5989 A mass spectrometer operated at 70 eV.

For flash pyrolysis, a Fischer 0316 Curie-point flash pyrolyser was used. Samples were pyrolysed for 10 s on a ferromagnetic wire with a Curie temperature of 610°C. The pyrolysis products were directly separated and analysed by GC/MS under the same conditions as described above.

2.5. GC–C–IRMS

Isotopic analyses of individual pyrolysis products using the GC–C–IRMS technique were performed using a HP 5890 gas chromatograph (50 m BPX 5 capillary column, i.d. 0.32 mm and film thickness of 0.25 μm; heating program 100 to 350°C at 3°C/min, splitless injector at

320°C) coupled to a CuO furnace (850°C), a cryogenic water trap, and a VG Optima mass spectrometer.

3. Results and discussion

3.1. Morphological and ultrastructural observations

3.1.1. Observation of thin sections by light microscopy

When observed under transmitted natural light (microscopic scale), the black shale appears to be composed of stacked organic-rich clay and carbonate microlayers (ca.100 μm in thickness). UV fluorescence observations reveal that, in the carbonate microlayers, the OM is only present in the internal structure of a few tests of planktonic forams. As a result, the OM in this black shale sample is almost entirely located in the organic-rich clay microlayers.

3.1.2. Scanning electron microscopy

SEM BSE observations on the organic-rich clay microlayers, coupled with X-ray measurements (pin-point chemical analyses and elemental mapping) confirm an intimate association between clay minerals and OM. Indeed, chemical mapping shows the superposition, at the scale of several micrometers, of OM (carbon mapping) and clay minerals (aluminium mapping) (Fig. 2). It should be noted that the OM particle in the central part of the picture is shown to illustrate the aspect of pure OM, but is not quantitatively important in our sample. In sharp contrast to the clay-rich microlayers, almost no OM is observed in the carbonate microlayers. In fact, as shown by SEM BSE, except for the few foraminifera tests, the carbonate is microcrystalline, resulting from re-precipitation. The authigenic origin of the carbonates is fully consistent with the lack of OM in these microlayers. Such a tight and exclusive association between clays and OM, down to a microscopic scale, is consistent with a major role of protection by clay minerals in OM preservation and kerogen formation. Moreover, anoxic conditions may also have favoured, in addition to the preservation by minerals, the organic matter preservation. A similar, direct association between OM and clay mineral grains was observed by SEM BSE in a quaternary sediment from Peru upwelling (Bishop et al., 1992).

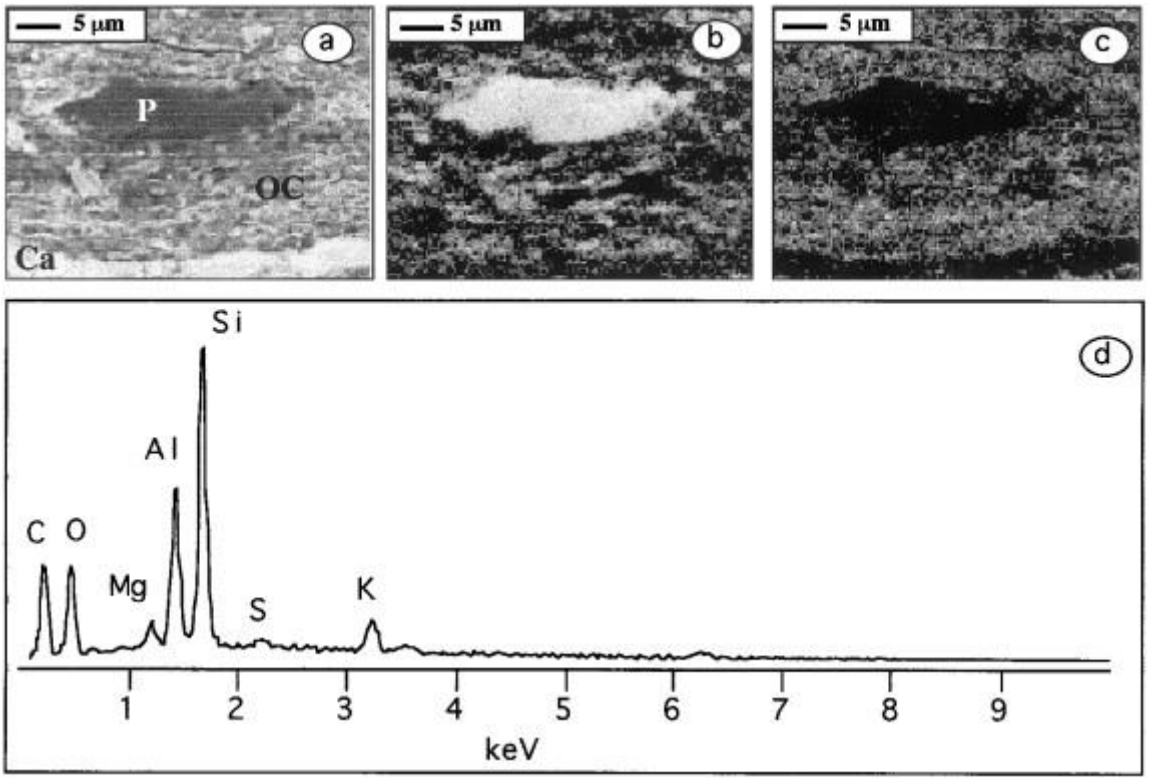

Fig. 2. (a) SEM BSE showing an organic particle (P), in fact a minor constituent of the bulk OM, and a microlayer of organic-rich clays (OC) overlying a calcium carbonate microlayer (Ca). Calcium mapping showed that no Ca is present in (OC) and (P). The carbon observed in both areas therefore corresponds to organic carbon. Elemental mapping, where white indicates the presence of an element and black indicates its absence, of carbon (b) and aluminium (c) reveals the intimate association of OM and clay minerals in (OC). EDS spectrum of pin-point analysis of (OC) (d) shows that, at this scale, signals of OM and clay minerals cannot be separated.

3.1.3. Transmission electron microscopy

TEM observations performed on ultrathin sections, perpendicular to the bedding plane, of the raw rock reveal that organic-rich clay microlayers are comprised of a succession of lens-shaped organic nanolayers (ca. 200 nm thick) parallel to the bedding. These layers are lined by lens-shaped clay mineral nanolayers of the same thickness. Some clay particles are dispersed in the organic nanolayers (Fig. 3). The latter probably correspond to the sedimentation of flocks comprising both OM and clay particles, as previously considered in recent sediments by Ransom 1997, Ransom et al, 1998a and Ransom 1998b) and by Boussafir et al. (1995) in ancient sediments from the Kimmeridge Clay Formation. The observed layering must be the consequence of compaction. HRTEM and electron micro-diffraction were performed on our sample in order to test the possible occurrence of OM within the clay mineral structure. Both micrographs and electron diffraction patterns (Fig. 4) show that the clay particles are very well crystallized with an interlayer spacing of 10 Å, which is a typical value for illites and other true micas. These HRTEM observations and electron micro-diffraction patterns therefore demonstrate that no OM is present within the clay structure, since occurrence of OM within the structure would expand the interlayer spacing.

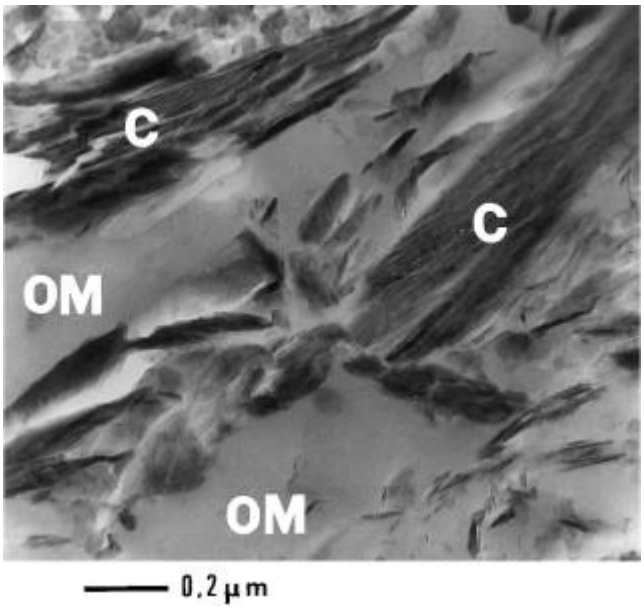

Fig. 3. TEM micrograph showing clay nanolayers lining organic matter nanolayers. (OM) is for organic matter and (C) for clay particles.

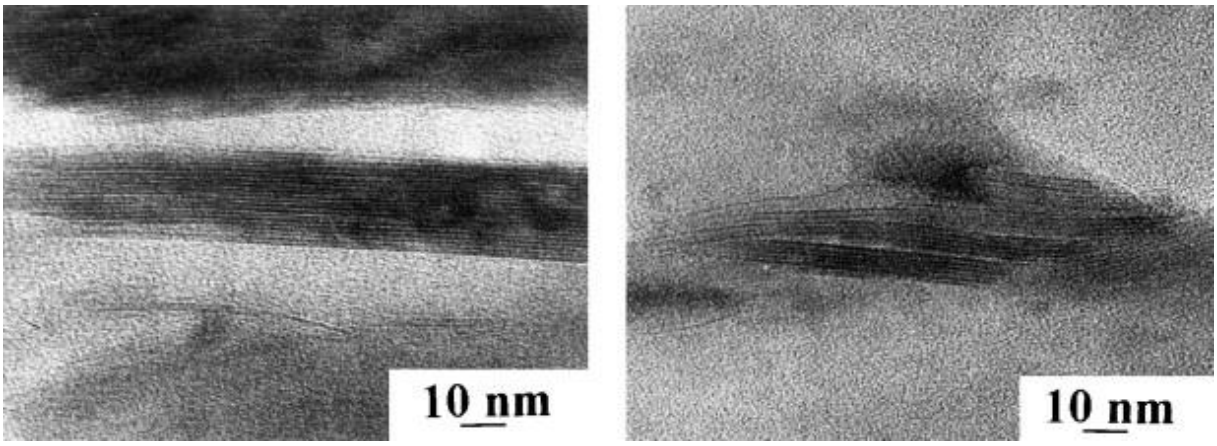

Fig. 4. HRTEM micrographs of clay particles showing interlayer distances (parallel lines inside of the particle).

X-ray pin-point analyses performed on the clay particles embedded in, or lining the OM nanolayers indicate that they belong to the illite group. These clay particles correspond to 25% of the total clay mineral content as revealed by bulk X-ray diffraction (J.F. Deconinck, pers. comm.). Ransom et al, 1998a and Ransom 1998b), in a study on Recent sediments from continental margins, observed a preferential association of the OM with clay minerals of the smectite group. If we consider the well-known diagenetic transformation of smectites into illites, the Ransom et al, 1998a and Ransom 1998b) observations and ours are consistent.

In the case of OM adsorption onto clay particles, such particles are expected to be coated with a very thin layer of OM (only a few nm). The highest known adsorption capacity of clay minerals thus corresponds to TOC values at most of ca. 7% (Keil et al., 1994a). Indeed, the

present observations at a nanoscopic scale indicate that the high amount of OM in the studied black shale (TOC=13.6%) cannot be merely explained by adsorption onto clay minerals. Rather, it appears that the role of clay particles in OM preservation is one of physical protection, resulting from the alternation of lens-shaped organic and clay nanolayers, rather than mere adsorption. We suggest that this form of association with clay particles resulted in OM being isolated in microenvironments where it could be protected against bacteria and their exoenzymes. In situ TEM observations of OM from continental margins led to similar conclusions. Ransom 1997, Ransom et al, 1998a and Ransom 1998b), who found that most organic matter appears to be associated with clay-rich domains with no uniform organic coating being observed on the grains, argued against the hypothesis of monolayer adsorption of OM onto mineral surfaces.

3.2. Chemical stability of isolated kerogen

Based on the intimate association between OM and clay minerals, we investigated the protective role of the associated minerals by removing the mineral matrix and monitoring the molecular-level composition of kerogen over rapid (1–2 years) time scales. To this end, the chemical structure of the isolated kerogen (via elimination of minerals by HF/HCl treatment) was examined just after isolation (ker-0) and after storage for one and two years (ker-1 and ker-2, respectively) (Fig. 1). The stability of the isolated kerogen was assessed from its bulk geochemical parameters and the composition of the corresponding pyrolysates (pyr-0, pyr-1 and pyr-2, respectively) determined by GC/MS analysis. In the same way, the kerogen which was isolated after 2 years of storage of the ground rock (ker-2bis) was studied immediately after isolation via flash pyrolysis (Fpyr-2bis).

3.2.1. Isolated kerogen

The FTIR and ^{13}C NMR spectra of ker-0 have been previously discussed (Salmon et al., 1997). Spectra of ker-1 and ker-2 are similar to those of ker-0. However, the progressive appearance of two absorption bands at 1210 and 1150 cm^{-1}, corresponding to C–O bonds, is apparent in the FTIR spectra upon storage (Fig. 5). In the ^{13}C NMR spectra (not shown) only a slight decrease in the relative intensity of the peak centred at 110 ppm and assigned to unsaturated carbons is observed in ker-2 when compared to ker-0. Taken together, these variations in the FTIR and ^{13}C NMR spectra with storage are consistent with some oxidative degradation of the kerogen. In agreement with NMR observations and with the well documented sensitivity of olefinic unsaturated bounds to oxygen incorporation, this degradation would especially affect C□C bonds. However, the occurrence of such oxidation processes cannot be directly demonstrated via elemental analysis (i) due to substantial ash levels, significant measurements cannot be carried out for oxygen and (ii) since the elimination of residual ash would require drastic treatments (e.g. with HNO_3) which would strongly alter the OM chemical structure.

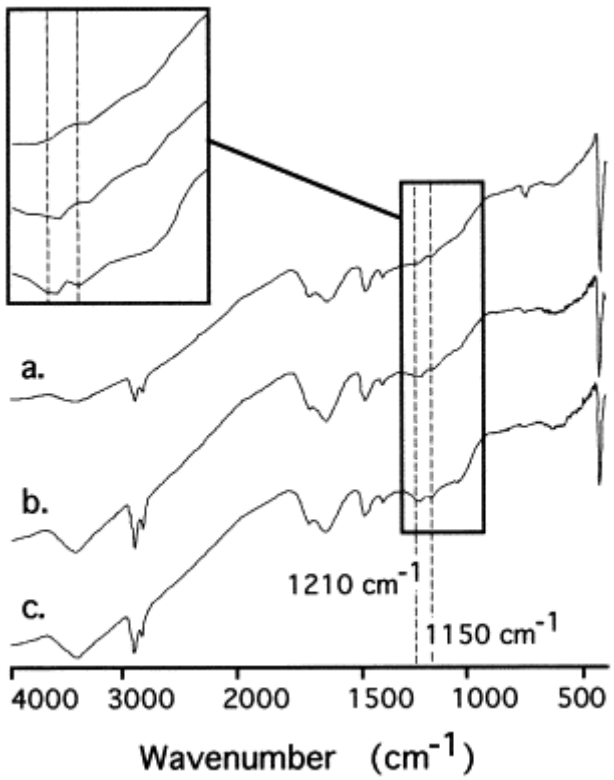

Fig.5. FTIR spectra of ker-0 (a), ker-1 (b) and ker-2 (c) showing the progressive increase of two bands at 1210 and 1150 cm^{-1} from ker-0 to ker-2.

Comparison of the mass balances of the 400°C pyrolysis of ker-0, ker-1 and ker-2 (Table 1) reveals a gradual rise, with storage duration, in the amount of volatile products, along with a drastic lowering in the amount of trapped and extracted compounds.

Table 1. Mass balances of the different fractions generated from ker-0, ker-1 and ker-2 *via* 400°C off-line pyrolysis, as wt% of the initial material

Sample	Lost[a]	Trapped[b]	Volatiles[c]	Extracted[d]	Residue[e]
ker-0	37.3	13.7	23.6	3.9	58.8
ker-1	37.6	9.2	28.4	3.8	58.6
ker-2	43.7	5.5	38.2	0.3	56.0

a

Total loss determined from the non-extracted pyrolysis residue; corresponds to trapped and volatile products.

b

Products dragged by the helium flow, with a molecular weight high enough to be trapped in chloroform at −5°C.

c

Products dragged by the helium flow, with a molecular weight too low to be trapped. This value was determined by difference between the total weight loss and the trapped products.

d

Cracking products with a low volatility, not dragged by the helium flow, extracted from the pyrolysis residue by organic solvents ($CHCl_3$/MeOH; 1/1; v/v).

e

Insoluble residue.

The composition of pyr-1 and pyr-2 as revealed by GC/MS was compared with that of pyr-0 (Fig. 6 and Fig. 7). The pyrolytic study of ker-0 (Salmon et al., 1997) indicated that the macromolecular network of this kerogen is mainly based on long, normal hydrocarbon chains but also comprises C_{40} isoprenoid chains with a lycopane skeleton. We therefore first investigated the influence of the storage of the isolated kerogen on these two types of chains.

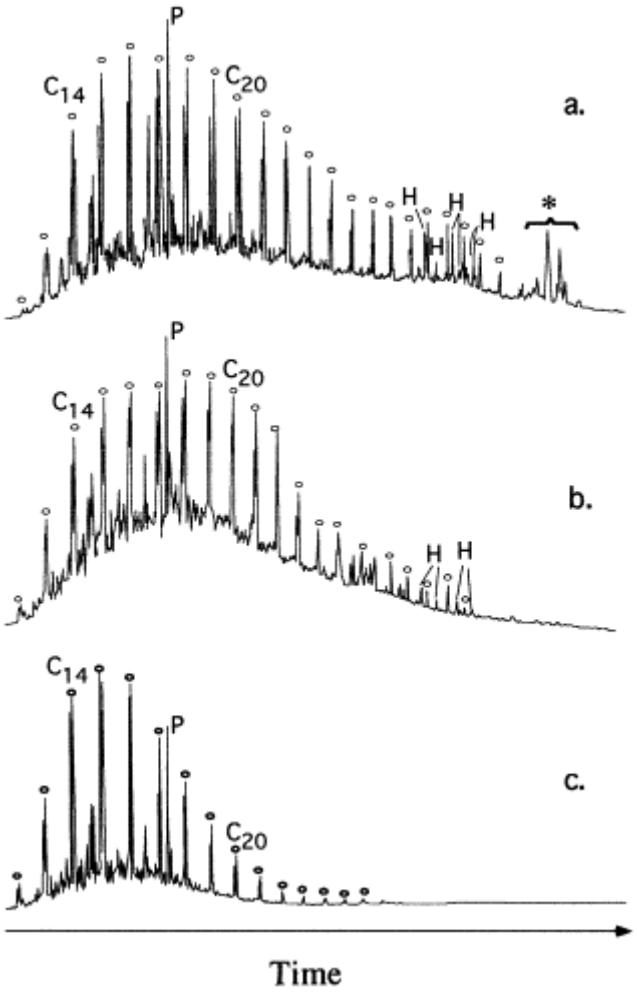

Fig. 6. GC traces and main components of the heptane-eluted fractions obtained via 400°C pyrolysis from the freshly isolated kerogen (a), kerogen after 1 year of storage (b) and 2 years of storage (c). o: *n*-alkane/*n*-alkene doublets (numbers refer to carbon chain length), P: prist-1-ene, H: hopanoids, *: C_{40} hydrocarbons derived from a lycopane skeleton.

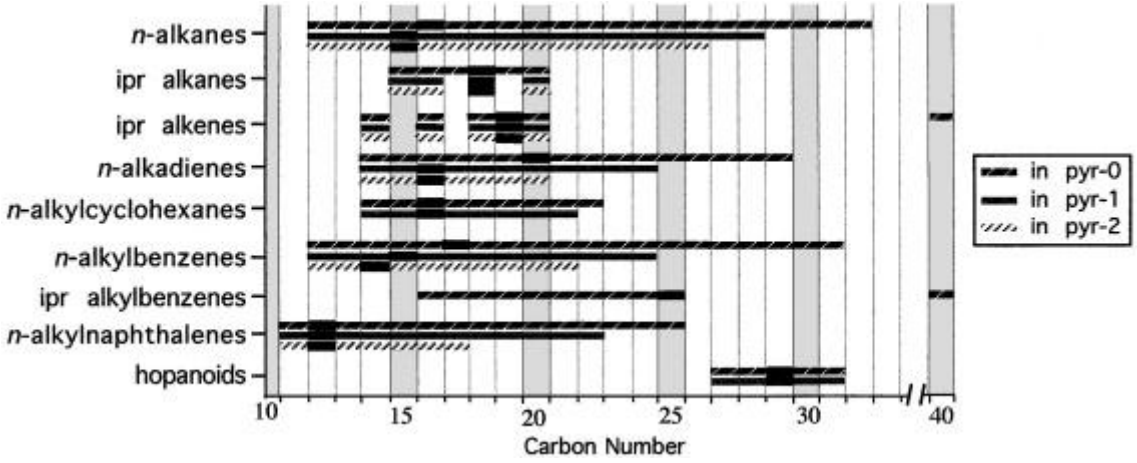

Fig. 7. Carbon number range and maximum (bold area) of the major series in the heptane-eluted fraction. Similar distributions were observed for *n*-alk-1-enes and *n*-alkanes. The absence of the line(s) corresponding to pyr-1 and/or pyr-2 indicates that the series was not detected in this(these) pyrolysate(s).

3.2.1.1. *n*-Alkyl chains

Pyrolysis of long *n*-alkyl chains is known to yield *n*-alkanes and *n*-alk-1-enes. These compounds are responsible for the predominant doublets in the GC traces of pyr-1 and pyr-2 but a progressive shift in the average chain length of the *n*-alkanes and *n*-alk-1-enes towards shorter chains is observed with storage duration (Fig. 6 and Fig. 7). For example, the maximum chain length of the *n*-alkanes shifts from C_{32} in pyr-0 to C_{26} in pyr-2 and a sharp decrease in the relative abundance of the C_{22}+ chains for pyr-1 and of the C_{16}+ chains for pyr-2 is observed (Fig. 6 and Fig. 7). A similar trend is observed via selective ion detection for less abundant series bearing *n*-alkyl chains such as *n*-alkadienes (*m/z*=67), *n*-alkylcyclohexanes (*m/z*=83), *n*-alkylbenzenes (*m/z*=91), *n*-alkylnaphthalenes (*m/z*=141) (Fig. 7) and also for *n*-alkan-2-ones (*m/z*=58), *n*-alkylphenols (*m/z*=107) and *n*-alkoxyphenols (*m/z*=109 and 124) (as illustrated for the ketones in Fig. 8a and b). This shortening of the *n*-alkyl chains is consistent with the above mentioned increase in the abundance of volatile products and with the parallel decrease in the contribution of trapped and extracted compounds in 400°C pyrolysis products, along with storage duration.

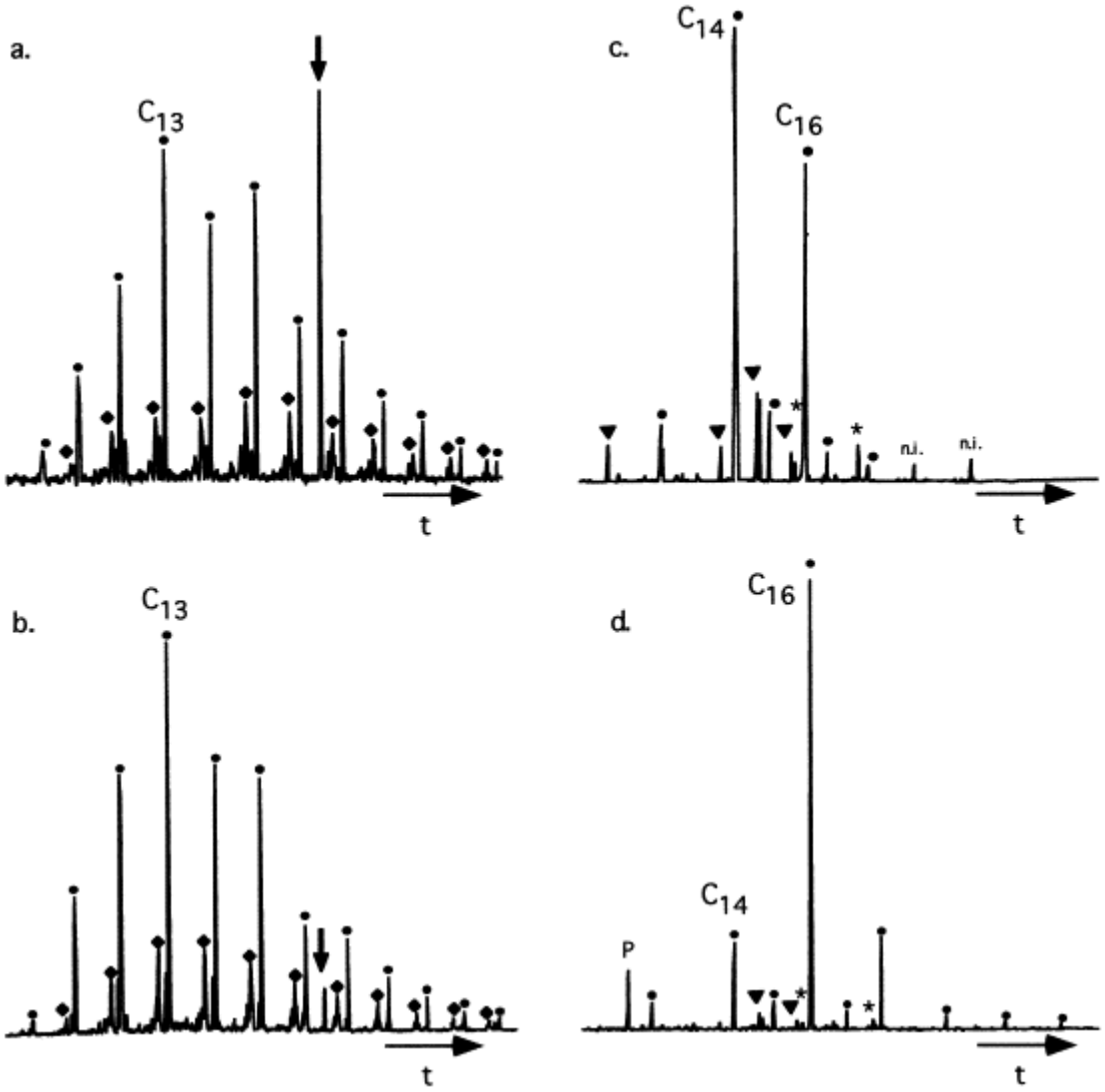

Fig. 8. Mass fragmentogram at *m/z*=58 for pyr-0 (a) and pyr-2 (b), showing the *n*-alkan-2-ones (•), the mid-chain ketones (♦) and a C18 isoprenoid ketone ( ), and Mass fragmentogram at *m/z*=74 for pyr-0 (c) and pyr-2 (d) showing the esterified saturated (•) and unsaturated (★) *n*-fatty acids and the esterified branched fatty acids (▾). n.i. are non identified products. Unsaturated abundance is strongly underestimated by detection at *m/z*=74.

3.2.1.2. Lycopane-related chains

Several series of compounds comprising isoprenoid chains were identified in substantial amount in pyr-0: C_{15}–C_{20} alkanes, $C_{14,}$ C_{16} and C_{18}–C_{20} alkenes, C_{16}–C_{25} alkylbenzenes, C_{18}–C_{22} ketones and C_{40} hydrocarbons and a ketone with a lycopane or lycopane-derived skeleton (Salmon et al., 1997). The occurrence of the latter C_{40} compounds reflects the contribution of lycopane-type chains to the macromolecular structure of the kerogen, and previous GC–C–IRMS studies pointed to an algal origin for such moieties. The relatively short C_{15} to C_{25} isoprenoid compounds identified in the pyrolysate of the black shale kerogen might also be derived from lycopane moieties. Indeed, all these C_{26}- hydrocarbons and ketones could originate from secondary thermal cleavages and be derived from the same units as the C_{40} hydrocarbons and ketone. This interpretation is in agreement with previous observations dealing with the pyrolysis products from resistant biomacromolecules and related kerogens

(Behar et al., 1995 and Derenne 1994). However, sharply different trends are noted among the isoprenoid compounds. The relative abundances of the C_{15}–C_{20} alkanes and alkenes only slightly decrease from pyr-0 to pyr-2, whereas the abundances of all the other above isoprenoid pyrolysis products are sharply lowered. In fact, apart from the C_{18} ketone, which was initially present in a very high relative abundance (Fig. 8a), these compounds are no longer detected in pyr-1 and pyr-2. Such contrasting behaviour suggests an origin from different types of moieties for both groups of isoprenoid products. This hypothesis was tested by GC–C–IRMS measurements performed on pyr-0. Since the pyrolysate corresponds to a highly complex mixture, these measurements were carried out on at least four compounds corresponding to each series in order to avoid possible errors related to co-elution. All the values obtained for a given series typically differ by <1‰. The shorter-chain isoprenoid alkanes and alkenes were shown to have a $\delta^{13}C$ value of about −48‰, whereas a value of about −29‰ was obtained for the C_{40} compounds. The $\delta^{13}C$ value of the former C_{15}–C_{20} products is close to the one obtained for hopanoids in ker-0 pyrolysate (ca. −42‰, Salmon et al., 1997), thus suggesting a chemoautotroph bacterial origin (Freeman et al., 1990). In contrast, the $\delta^{13}C$ values and degradation rates suggest a common origin from algal-derived moieties with a lycopane skeleton, for the alkylbenzenes, the C_{18}–C_{22} and C_{40} ketones, and the C_{40} hydrocarbons. These moieties, based on a lycopane skeleton and of algal origin, exhibit a high level of alteration with storage, as reflected by the almost complete disappearance of their pyrolysis products in pyr-1 and pyr-2. This result is in agreement with the previously demonstrated lability of such long isoprenoid chains (Behar et al., 1995 and Derenne 1994). In contrast, the C_{26}- isoprenoid alkanes and alkenes of bacterial origin seem to derive from structures which are more resistant to oxidative degradation.

3.2.1.3. Hopanoids

Hopanoids are known to occur as bound units in kerogens (Innes et al., 1997 and Ourisson 1979) and a relatively large amount of these polycyclic terpenic products is indeed observed in ker-0 pyrolysate (Fig. 6a). A marked decrease in the proportion of these compounds is noted with storage, as indicated by a decrease in the relative abundance of the hopanoids with respect to the *n*-alkanes (relative abundance is calculated as the ratio of the most abundant hopanoid over the most abundant *n*-alkane) from 0.27 in pyr-0, 0.18 in pyr-1 to undetectable in pyr-2.

3.2.1.4. Fatty acids

Fatty acids in pyrolysates result from the thermal cleavage of ester functions. Their nature and distribution are commonly used as indices of kerogen alteration. As previously discussed (Salmon et al., 1997), the fatty acid composition in pyr-0, is similar to that from living organisms, and reveals a low level of degradation (strong even-over-odd predominance, important contribution of unsaturated compounds). A sharp decrease in the unsaturated acids (31 to 1% of total acids in pyr-0 and pyr-2, respectively) is observed during storage. Although the corresponding acid moieties linked as esters exhibited a high stability on a geological time scale in the whole rock (as evidenced by their low level of alteration in pyr-0) they appear highly sensitive to degradation after elimination of the mineral matrix. In addition, the appearance of long chain fatty acids up to C_{24} was noted in pyr-2 (Fig. 8c and d). The formation of these acids may reflect the oxidation of some alkyl chains in the macromolecular structure of the kerogen upon storage. Production of carboxylic acids upon oxidation of *n*-alkyl side chains was previously reported in high molecular weight constituents of crude oils (Duhaut et al., 1997).

Taken together, all the above data point to a fast alteration of the chemical structure of this black shale kerogen after isolation from the mineral matrix. Such a fast degradation is most likely related to oxidation processes as suggested by changes in spectroscopic features and pyrolysate composition upon storage. Indeed, (i) the shortening of chain-length of the trapped products, along with the progressively rising amount of volatile products in pyr-1 and pyr-2, (ii) the appearance of C–O bonds during storage of the kerogen as observed by FTIR and (iii) the appearance of long chain fatty acids all strongly imply the occurrence of oxidative processes. These processes would result in an increase in the amount of cross-linkages within the macromolecular structure, thus shortening some of the alkyl chains. It therefore appears that potentially labile OM in this black shale was preserved on a geologic scale, due to association with minerals. This mechanism may exhibit similar results to those obtained with Recent sediments in which it was demonstrated that sedimentary OM was rapidly remineralized once desorbed (Keil et al., 1994b). It was concluded in this latter study that intrinsically labile biochemicals may be preserved by adsorption onto minerals. Although OM and clay minerals in the cenomanian black shale are intimately associated at a micrometric scale (BSEM observations), TEM observations show that OM is not adsorbed on clays, but predominantly occurs as lens-shaped discrete organic layers. We conclude that the efficient protective role of the minerals is probably via physical protection with the OM.

3.2.2. Ground rock

Rock-Eval pyrolysis carried out on ground rock sample after 2 years of storage showed that the amount (TOC) and hydrogen index of the OM in the ground rock was not altered during storage. However, a significant increase in the Oxygen Index was observed, from 9 mg CO_2/mg TOC in the initial material to 30 mg CO_2/g TOC after 2 years. FTIR and ^{13}C NMR spectra of the kerogen isolated from the above sample (ker-2bis) are analogous to those of ker-0.

Due to the low amount of ker-2bis available, this sample was analysed by Curie-point flash pyrolysis. So as to compare these results with those described above, which were obtained via off-line pyrolysis, ker-2 was also analysed by Curie-point Py/GC/MS. Comparison of the distributions of ker-2 pyrolysis products obtained by both pyrolytic methods indicates that the carbon number range of the different series (i) is wider for the on-line measurements, as expected, due to the loss of volatile products in the off-line pyrolysate but (ii) extends up to similar chain length (e.g. maximum carbon number of 26 for the *n*-alkanes in the flash pyrolysate versus 26 in off-line pyrolysis). It should be emphasized that, as indicated previously in the experimental section, the fatty acids in the off-line pyrolysate were derivatized into methyl esters in order to enhance their detection. Indeed, no C_{18}+ fatty acid could be directly detected under our GC conditions. For the flash pyrolysate, however, the derivatization was not possible. Therefore, no comparison could be achieved for the fatty acids released upon the two types of pyrolysis. The relative abundances of all the other pyrolysis compounds with respect to the *n*-alkanes are similar in off-line and flash pyrolysates of ker-2. As a result, the maximum carbon number, as well as the relative abundances of these series, observed in the flash pyrolysate of ker-2bis (Fpyr-2bis), can be directly compared with those from the off-line pyr-0, -1 and -2.

3.2.2.1. *n*-Alkyl chains

In Fpyr-2bis, *n*-alkane/*n*-alk-1-ene doublets extend up to C_{29} (Fig. 9). This maximum chain length is longer than that observed in pyr-2 (C_{26}) and substantially shorter than in pyr-0. The

contribution of the C_{16}+ chains in Fpyr-2bis is also intermediate between pyr-0 and pyr-2. The shortening of the alkyl chains in the pyrolysis products from pyr-0 to pyr-2 was discussed above and was shown to reflect the alteration of the corresponding kerogen.

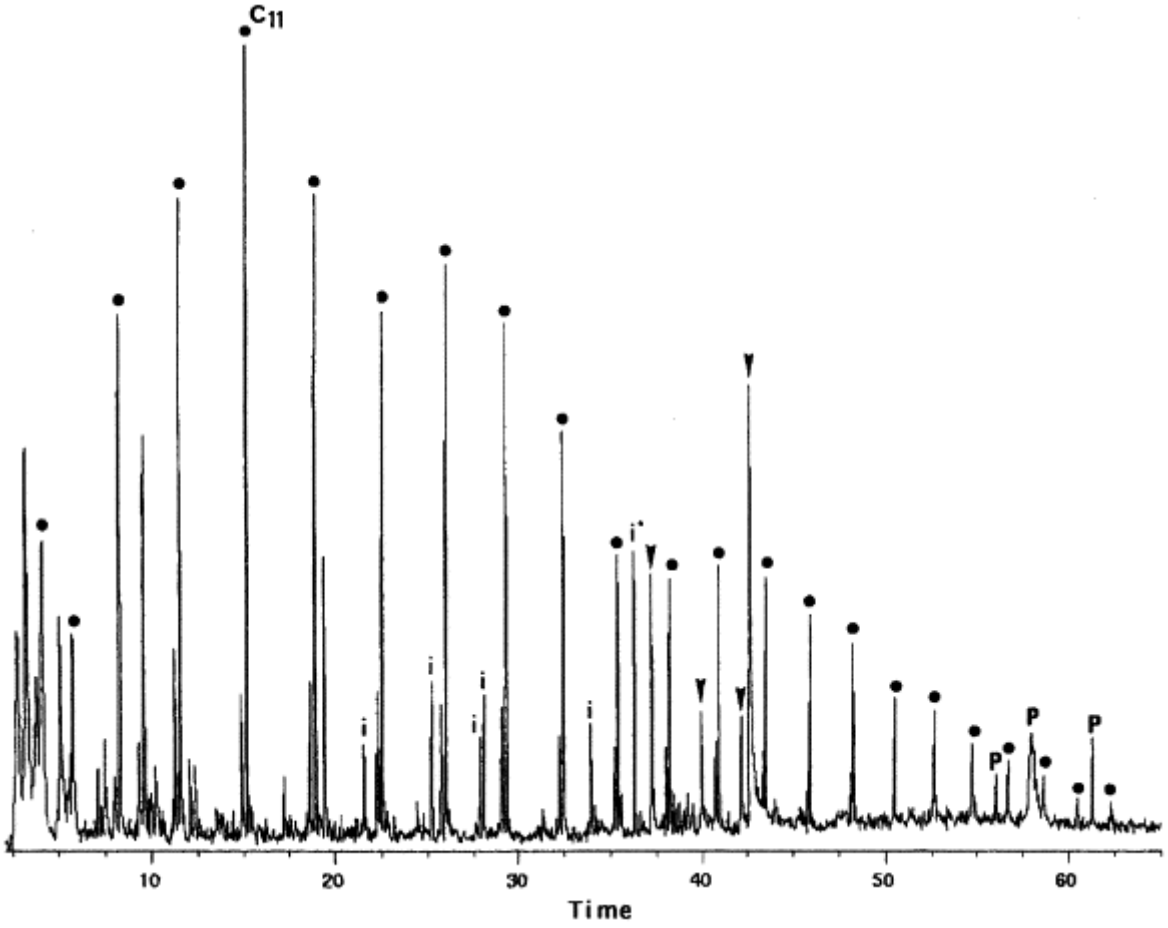

Fig. 9. Mass fragmentogram at *m/z*=57 of Fpyr-2bis, flash pyrolysate of the kerogen isolated from the ground rock stored for 2 years, showing the distributions of the *n*-alkanes (•), C_{18}-C_{22} isoprenoid alkanes and alkenes (i) (prist-1-ene is noted i*) and fatty acids (‰). P is for contaminants.

3.2.2.2. Lycopane-related compounds

No C_{40} compound could be detected in Fpyr-2bis, nor C_{18}–C_{22} isoprenoid ketones or alkylbenzenes. Again, this illustrates the high lability of algal-derived moieties with a lycopane-type skeleton, from which these compounds are derived. In contrast, C_{15}–C_{20} isoprenoid alkanes and alkenes are present. As previously discussed, the latter isoprenoid compounds, probably of bacterial origin, are derived from moieties more resistant to oxidative degradation than lycopane-type ones.

3.2.2.3. Hopanoids

Hopanoids are detected in Fpyr-2bis by mass fragmentograms at *m/z*=191 and they exhibit the same distribution as in pyr-0. Whereas no hopanoids were detected in the off-line

pyrolysate of ker-2, they could be detected in the corresponding flash pyrolysate, but only in very low relative abundance (less than 0.01). The relative abundance of the hopanoids (calculated as indicated in a previous section) in Fpyr-2bis (0.10) is significantly lower than in pyr-0 (0.27), and similar to pyr-1 (0.11). Such differences also indicate a degree of degradation for ker-2bis which is intermediate between those of ker-0 and ker-2.

It thus appears that during 2 years of storage, the OM in the ground rock underwent some alteration, but the extent of the latter was not as important as for the isolated kerogen after the same storage duration. This observation is consistent with the physical protection model deduced from TEM observations since, after grinding, the OM was partly exposed to air but also still partly protected within the mineral matrix, hence it experienced an intermediate level of degradation when compared to the isolated kerogen.

4. Conclusion

This study, combining microscopic and pyrolytic methods on a Cenomanian black shale, to the best of our knowledge, provides the first direct indications for a major role of minerals in OM protection in a sedimentary rock. The OM appears to have been physically protected by clays. Adsorption on the mineral phase possibly played a role, however the alternation of OM and clay nanolayers observed by electron microscopy suggest a physical protection mechanism. Moreover, clays are known for their catalytic properties, and condensation reactions of the associated OM, leading to kerogen formation, were likely favoured by this mineral phase.

Even after 90 Myears, physical protection by clay minerals appears to remain important, as evidenced by the instability of the isolated kerogen within 2 years of storage. This last result indicates that ancient macromolecular OM, although it is commonly considered as a highly inert material, remains sensitive to oxygen-mediated physico-chemical alterations. Due to this unexpected lability, it appears necessary to exercise caution in order to avoid misinterpretation in kerogen structures and derived information on depositional environment, when isolated kerogen samples are analyzed.

Acknowledgements

We wish to thank Dr. M. Boussafir (Orléans University) for providing advice in preparations of in-situ organic matter for TEM. We would like to thank C. Clinard (CNRS, Orléans) who provided assistance in HRTEM observations. We are grateful to Professor A. Mariotti (Paris VI University) who enabled the GC–C–IRMS analyses to be performed in his laboratory, and to G. Bardoux who performed them. We also thank Y. Pouet (ENSCP Paris) for performing GC/MS analyses as well as combined Py/GC/MS. Dr. F. Baudin (Paris VI University) and Dr. J.R. Disnar (Orléans University) are thanked for providing Rock-Eval data.

References

Beadoin et al., 1996
Beaudoin, B., M'Ban, E. P., Montanari, A., Pinault, M., 1996. Lithostratigraphie haute résolution (<20 ka) dans le Cénomanien du bassin d'Ombrie-Marches (Italie). Comptes Rendus de l'Académie des Sciences Paris 323 IIa, pp. 689–696.

Behar et al., 1995
F Behar, S Derenne, C Largeau

Closed pyrolyses of the isoprenoid algaenan of *Botryococcus braunii*, L race. Geochemical implications for derived kerogens
Geochimica et Cosmochimica Acta, 59 (1995), pp. 2983–2997

Bergamashi et al., 1997
B.A Bergamashi, E Tsamakis, R.G Keil, T.I Eglinton, D.B Montluçon, J.I Hedges
The effect of grain size and surface area on organic matter, lignin and carbohydrate concentration, and molecular composition in Peru Margin sediments
Geochimica et Cosmochimica Acta, 61 (1997), pp. 1247–1260

Bishop et al, 1992
A.N Bishop, J.T Westrich, R.L Patience
Analysis of sedimentary organic matter by scanning electron microscopy: the application of back-scattered electron imagery and light element X-ray microanalysis
Organic Geochemistry, 18 (1992), pp. 431–446

Boussafir et al, 1994
Boussafir, M., Lallier-Vergès, E., Bertrand, P., Badaut-Trauth, D., 1994. Etude ultratructurale de matières organiques microprélevées dans les roches de la "Kimmeridge Clay Formation" (Yorkshire, UK). Bulletin du Centre de Recherches Exploration Production Elf Aquitaine Publication Speciale 18, 275–277.

Boussafir et al., 1995
M Boussafir, F Gelin, E Lallier-Vergès, S Derenne, P Bertrand, C Largeau
Electron microscopy and pyrolysis of kerogens from the Kimmeridge Clay Formation, UK.: source organisms, preservation processes and origin of microcycles
Geochimica et Cosmochimica Acta, 59 (1995), pp. 3731–3747

Collins
M.J Collins, A.N Bishop, P Farrimond
Sorption by mineral surfacesrebirth of the classical condensation pathway for kerogen formation?
Geochimica et Cosmochimica Acta, 59 (1995), pp. 2387–2391

Degens et al., 1984
E.T Degens, V Ittekkot
A new look at clay–organic interactions
Miteilungen des Geologisch-Paläontologischen Institutes der Universität Hamburg, 56 (1984), pp. 229–248

Derenne 1994
S Derenne, C Largeau, F Behar
Low polarity pyrolysis products of Permian to Recent Botryococcus-rich sedimentsfirst evidence for the contribution of an isoprenoid algaenan to kerogen formation
Geochimica et Cosmochimica Acta, 58 (1994), pp. 3703–3711

Duhat et al., 1997
Duhaut, A., Lemoine, S., Adam, P., Berrut, J.-B., Connan, J., Albrecht, P., 1997. Structural modification of geomacromolecules induced by oxidation of crude oil under

natural conditions. In: Abstracts 18th International Meeting on Organic Geochemistry, Maastricht, The Netherlands, Forschungszenbrum, Jülich, pp. 95–96.

Durand 1980
B Durand, G Nicaise
Procedures for kerogen isolations
B.(Ed.) Durand (Ed.)Kerogen. Technic, Paris (1980), pp. 35–53

Freeman et al., 1990
K.H Freeman, J.M Hayes, J.-M Trendel, P Albrecht
Evidence from carbon isotope measurements for diverse origins of sedimentary hydrocarbons
Nature, 343 (1990), pp. 254–256

Innes et al., 1997
H.E Innes, A.N Bishop, I.M Head, P Farrimond
Preservation and diagenesis of hopanoids in Recent lacustrine sediments of Priest Pot, England
Organic Geochemistry, 26 (1997), pp. 565–576

Keil et al., 1994a
R.G Keil, E Tsamakis, C.B Fuh, J.C Giddings, J.I Hedges
Mineralogical and textural controls on the organic composition of coastal marine sedimentshydrodynamic separation using SPLITT-fractionation
Geochimica et Cosmochimica Acta, 58 (1994), pp. 879–894

Keil et al., 1994b
R.G Keil, D.B Montluçon, F.G Prahl, J.I Hedges
Sorptive preservation of labile organic matter in marine sediments
Nature, 370 (1994), pp. 549–552

Largeau et al., 1986
C Largeau, S Derenne, E Casadevall, A Kadouri, N Sellier
Pyrolysis of immature Torbanite and of the resistant biopolymer (PRB A) isolated from extant alga *Botryococcus braunii.* Mechanism of formation and structure of Torbanite
D Leythaeuser, J Rullkötter (Eds.), Advances in Organic Geochemistry 1985, Organic Geochemistry 10. Pergamon Press, Oxford (1986), pp. 1023–1032

Mayer et al, 1985
L.M Mayer, P.T Rahaim, W Guerin, S.A Macko, L Watling, F.E Anderson
Biological and granulometric controls on sedimentary organic matter of an intertidal mudflat
Estuarine Marine and Coastal Shelf Science, 20 (1985), pp. 491–503

Mayer et al., 1988
L.M Mayer, S.A Macko, L Cammen
Provenance, concentration and nature of sedimentary organic nitrogen in the Gulf of Maine
Marine Chemistry, 25 (1988), pp. 291–304

Mayer 1994a
L.M Mayer

Surface area control on organic carbon accumulation in continental shelf sediments
Geochimica et Cosmochimica Acta, 58 (1994), pp. 1271–1284

Mayer 1994b
L.M Mayer
Relationships between mineral surfaces and organic carbon concentrations in soils and sediments
Chemical Geology, 114 (1994), pp. 347–363

Ourisson 1979
G Ourisson, P Albrecht, M Rohmer
The hopanoids, paleochemistry and biochemistry of a group of natural products
Pure and Applied Chemistry, 51 (1979), pp. 709–729

Ransom 1997
B Ransom, R.H Bennett, R Baerwald
In situ organic matter in recent marine sedimenta TEM investigation of organic matter preservation on continental margins and the monolayer hypothesis
Marine Geology, 138 (1997), pp. 1–9

Ransom et al, 1998a
B Ransom, D Kim, M Kastner, S Wainwright
Organic matter preservation on continental slopesimportance of mineralogy and surface area
Geochimica et Cosmochimica Acta, 62 (1998), pp. 1329–1345

Ransom 1998b
B Ransom, K.F Shea, P.J Burkett, R.H Bennett, R Baerwald
Comparison of pelagic and nepheloid layer marine snowimplications for carbon cycling on the California margin
Marine Geology, 150 (1998), pp. 39–50

Salmon et al., 1997
V Salmon, S Derenne, C Largeau, B Beaudoin, G Bardoux, A Mariotti
Kerogen chemical structure and source organisms in a Cenomanian organic-rich black shale (Central Italy) — indications for an important role of the “sorptive protection” pathway
Organic Geochemistry, 27 (1997), pp. 423–438

Schlanger & Jenkyns 1976
S.O Schlanger, H.C Jenkyns
Cretaceous oceanic anoxic events: causes and consequences
Geologie en Mijnbouw, 55 (1976), pp. 179–184

Sinninghe Damste et al., 1989
J.S Sinninghe Damsté, T.I Eglinton, J.W Leeuw, P.A de Schenck
Organic sulphur in macromolecular organic matter. I. Structure and origin of sulphur-containing moieties in kerogen, asphaltenes and coals as revealed by flash pyrolysis
Geochimica et Cosmochimica Acta, 53 (1989), pp. 873–889

Suess 1973
E Suess
Interaction of organic compounds with calcium carbonate, II. Organo-carbonate associations in recent sediments
Geochimica et Cosmochimica Acta, 37 (1973), pp. 2435–2447

Tanoue & Handa 1979
E Tanoue, N Handa
Differential sorption of organic matter by various sized sediments particles in Recent sediment from the Bering Sea
Journal of the Oceanographic Society of Japan, 35 (1979), pp. 199–208

Tegelaar et al., 1989
Tegelaar, E.W., Leeuw, J.W. de, Derenne, S., Largeau, C., 1989. A reappraisal of kerogen formation. Geochimica et Cosmochimica Acta 53, 3103–3106.

Tissot 1984
B.P Tissot, D.H Welte
Petroleum, Formation and Occurrence
Springer, Berlin (1984)